JOURNAL OF MAGNETIC RESONANCE **135,** 522–528 (1998)
ARTICLE NO. MN981597

Modeling of Self-Diffusion and Relaxation Time NMR in Multi-Compartment Systems

Eugene G. Novikov,* Dagmar van Dusschoten,† and Henk Van As†,[1]

*Department of Systems Analysis, Belarusian State University, Minsk, Belarus; and †Wageningen Agricultural NMR Centre, Laboratory of Molecular Physics, Wageningen Agricultural University, Wageningen, The Netherlands

Received March 27, 1998; revised September 1, 1998

The theory of pulsed field gradient (pfg) NMR applied to molecules in cellular systems which contain different subcellular compartments separated by permeable membranes, acting as diffusion barriers, has been extended. A numerical model of restricted diffusion and magnetization relaxation behavior in pfg-CPMG NMR experiments, based on the Fick's second law of diffusion, is presented. This model is applicable to a wide range of systems and allows the exploration of temporal and spatial behavior of the magnetization with and without the influence of gradient pulses. Results of the numerical experiments show their correspondence to the previously observed ones and demonstrate the importance of the inclusion of the time domain data in analyzing diffusion measurements.

Key Words: **NMR; diffusion and time relaxation; numerical modeling; Fick's second law of diffusion.**

1. INTRODUCTION

Pulsed field gradient (pfg) NMR methods are very well suited to the study of relaxation and diffusion behavior of fluids in porous and biological media. In recent years pfg NMR has gained considerable attention by several groups (*1–3*). This is caused by technical improvements of the (active shielded) gradient sets, which allow for much more accurate pfg NMR measurements, and by new theoretical developments started by Kärger and Heink (*4*) and later Cory and Garroway (*5*) and Callaghan (*6*). Another factor contributing to the increase of pfg NMR studies and development of theories was the availability of proper model systems, e.g., polystyrene spheres (*6*).

When applied to biological systems containing different subcellular compartments and cell-to-cell transfer, interpretation of the pfg measurements becomes very complicated. Membranes can restrict diffusion but allow exchange and transport between the compartments which can have totally different relaxation behavior. This causes the observed results to be dependent on microstructure, membrane permeability, diffusion, and relaxation behavior in the different compartments. A number of theoretical models have been presented to interpret the diffusion and relaxation time measurements in such systems. Among these models three main branches can be identified: simulation models, analytical models based on the scattering wave-vector formalism, and analytical models based on the evaluation of Fick's second law of diffusion.

In simulation models (*7–9*) the position and spin orientation for every molecule in a system are numerically calculated for each time step. Since a random displacement vector representing the result of the collisions of the molecule with its surroundings and its phase shift caused by diffusion during the time step (which should be sufficiently small) is known, it is possible to follow all spin transformations in the given time and space regions in detail. This procedure is repeated for every molecule in the system. Various geometry configurations, types of molecular interactions, and shapes of magnetization pulses can be explored in this way. However, to get satisfactory statistical accuracy, thousands of molecular trajectories must be simulated, which may require hours or even days of calculations on powerful workstations. This approach, nevertheless, was implemented for the investigation of the validity of the short-gradient-pulse approximation in a planar (*7*), cylindrical and spherical geometry (*8*).

According to the scattering wave-vector formalism, the pfg echo amplitude represents a Fourier transform of the displacement propagator $P(x|x', \Delta t)$, which is the conditional probability that a spin starting at position x' will be found at position x after the time interval Δt. This approach has been introduced by Stejskal and Tanner (*10*) and was later adapted by several authors (*1, 11–15*). However, the diffusion propagator can be found only for a limited set of initial and boundary conditions in the so-called narrow-gradient-pulse approximation. Therefore, in most cases only one compartment is investigated (for example, (*1, 11*)), sometimes with the introduction of outside influencing compartments, which, however, need to be invisible for NMR (*12*). Also some efforts have been made to avoid limitations caused by the narrow-gradient-pulse approximation (*13, 14, 16*). Multi-compartment interconnected systems are far too complex to be described in the framework of the given

[1] To whom correspondence should be addressed. Fax: +31-317-482725. E-mail: henk.vanas@water.mf.wau.nl.

1090-7807/98 $25.00

approach. It is also hardly possible to extract relaxation effects of the diffusion system by propagator imaging.

The third branch of models, and probably the most promising, is based on the evaluation of Fick's second law of diffusion (*17*). For a given geometry this is a partial differential equation with respect to the local spin magnetization, which can be solved either analytically or numerically. This equation was used for the exploration of T_2 relaxation processes (*2, 18, 19*) and the influence of magnetic field gradient pulses on diffusing particles (*2, 11, 12*). Differential equation models allow for the investigation of a variety of systems with complicated configurations by changing the boundary conditions, or inserting functions, properly describing the shape of the magnetic field, etc. However, analytical solutions of the partial differential equation can only be found for a certain combination of initial and boundary conditions, and become difficult in common situations. Probably the best way out of this problem is to solve this differential equation numerically (*2, 20*). This way could be very fruitful from a practical point of view since numerical solutions let us explore a wide range of different systems and obtain results quickly.

In this paper we present further development of the numerical solution of Fick's second law of diffusion for multicompartment systems, which is applicable to a wide range of systems and allows us to explore the temporal behavior of magnetization with and without influence of gradient pulses. This is particularly important in view of recent developments of multiple spin echo pfg NMR pulse sequences (*21*), which let one measure the magnetization decay versus the echo time (t_e) and gradient strength (G) simultaneously. The design of the model roughly corresponds to the developed experimental setup and can easily be adopted to investigate the influence of different instrumental distortions and internal field gradients on the detected signal and to explore more complicated geometries of the compartments (nonplanar barriers).

In addition, we present some numerical results to show their correspondence to results obtained by other models and to demonstrate the importance of the time domain in diffusion measurements.

2. THEORY

We are investigating the behavior of magnetization in a one-dimensional system (Fig. 1), consisting of a set of compartments, separated by planar barriers. Each compartment is characterized by the decay time T_i, diffusion coefficient D_i, and length of the compartment L_i, surrounded by the membranes with the permeability parameters ρ_{i-1} and ρ_i. It was assumed that the width of the membranes is much smaller than the length of the compartments. The output boundaries are also characterized by the permeability values ρ_0 and ρ_n.

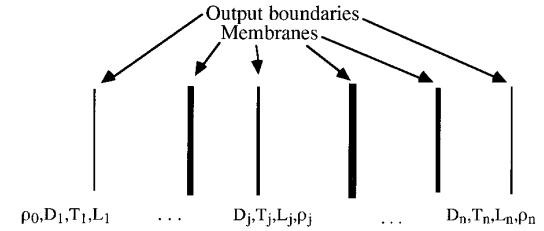

FIG. 1. Schematic presentation of a system consisting of compartments separated by permeable planar membranes.

The local spin magnetization $S(x, t)$ in such a system can be described by the following differential equation based on Fick's second law of diffusion (*17*):

$$\frac{\partial}{\partial t} S(x, t) = \frac{\partial}{\partial x}\left\{D(x)\frac{\partial}{\partial x} S(x, t)\right\} - \frac{1}{T(x)} S(x, t); \quad [1]$$

here $D(x)$ and $T(x)$ represent the diffusion coefficient and relaxation time, respectively, as functions of space coordinate. In our case diffusion and relaxation time remain constant within a particular compartment, but may differ for different compartments.

The influence of limited membrane permeability can be taken into account by posing proper boundary conditions, which for the left and right membranes of the jth compartment are written as

$$\rho_{j-1}[S_j(l_{j-1}, t) - S_{j-1}(l_{j-1}, t)] = D(l_{j-1})\frac{\partial S_j(l_{j-1}, t)}{\partial x},$$

$$\rho_j[S_{j+1}(l_j, t) - S_j(l_j, t)] = D(l_j)\frac{\partial S_j(l_j, t)}{\partial x},$$

$$l_0 = 0, \quad l_j = l_{j-1} + L_j, \quad j = 1, \ldots, n, \quad [2]$$

where $S_j(x, t) = S(x, t)$, $x \in [l_{j-1}; l_j]$, $j = 1, \ldots, n$, and n equals the total number of compartments. For the output boundaries we have

$$S_0(l_0, t) = F_0(t); \quad S_{n+1}(l_n, t) = F_1(t), \quad [3]$$

where $F_0(t)$ and $F_1(t)$ describe the behavior of the outer magnetization. Magnetization at time 0 (initial condition) takes the form

$$S(x, t_0) = f(x), \quad [4]$$

where $f(x)$ determines the initial distribution of the magnetization.

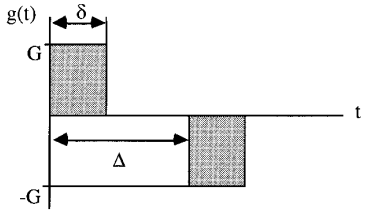

FIG. 2. Sequence of magnetic field gradient pulses.

In pfg NMR experiments, the amount and phase of the magnetization are influenced by the sequence of magnetic field gradient pulses. The partial differential equation [1] for the magnetization, including magnetic field gradients, takes the form (*19*, *20*)

$$\frac{\partial}{\partial t} S(x, t) = \frac{\partial}{\partial x}\left\{D(x)\,\frac{\partial}{\partial x} S(x, t)\right\} + \left(\sqrt{-1}\gamma g(t) x - \frac{1}{T(x)}\right) S(x, t), \qquad [5]$$

where $g(t)$ is the magnetic field gradient function and γ is the gyromagnetic ratio. In our calculations the function $g(t)$ is represented by a pair of magnetic field gradient pulses of duration δ separated by Δ, as shown in Fig. 2. These pulses have identical amplitude G, but opposite polarity.

The numerical solution of the partial differential equation is based on the transformation of Eq. [5] to an equation in finite differences. There are two different methods of transformation, according to either the implicit or the Crank–Nicholson scheme (*22*). Both schemes are stable for arbitrary values of the time step. Following the implicit scheme, the partial differential equation takes the form

$$\frac{S(x_i, t_k) - S(x_i, t_{k-1})}{\Delta t} = [D(x_i)(S(x_{i+1}, t_k) - S(x_i, t_k)) - D(x_{i-1})(S(x_i, t_k) - S(x_{i-1}, t_k))]/\Delta x^2 + \left(\sqrt{-1}\gamma g(t_k) x_i - \frac{1}{T(x_i)}\right) S(x_i, t_k),$$
$$k = 1, \ldots; \quad i = 0, \ldots, m, \qquad [6]$$

where $S(x_i, t_0) = f(x_i)$; $x_0 = l_0$, $x_m = l_n$; m is the number of space steps, and Δx and Δt represent the space and time discretization steps respectively. The Crank–Nicholson scheme of the transformation results in the following equation in finite differences:

$$\frac{S(x_i, t_k) - S(x_i, t_{k-1})}{\Delta t} = [D(x_i)(S(x_{i+1}, t_k) - S(x_i, t_k)) - D(x_{i-1})(S(x_i, t_k) - S(x_{i-1}, t_k)) + D(x_i)(S(x_{i+1}, t_{k-1}) - S(x_i, t_{k-1})) - D(x_{i-1}) \times (S(x_i, t_{k-1}) - S(x_{i-1}, t_{k-1}))]/2\Delta x^2 + \left(\sqrt{-1}\gamma g(t_k) x_i - \frac{1}{T(x_i)}\right) S(x_i, t_k), \qquad [7]$$

Taking into account boundary conditions [2] and [3], we have

$$D(x_i) = D_j,\ x_i \in (l_{j-1};\ l_j);$$
$$D(l_{j-1}) = \rho_{j-1}\Delta x; \quad D(l_j) = \rho_j \Delta x;$$
$$T(x_i) = T_j,\ x_i \in [l_{j-1};\ l_j]; \quad j = 1, \ldots, n$$
$$S(x_{-1}, t_k) = F_0(t_k); \quad S(x_{m+1}, t_k) = F_1(t_k). \qquad [8]$$

Such an interpretation of boundary conditions leads to the representation of each membrane as an additional compartment of length Δx with the diffusion coefficient $\rho\Delta x$, similar to earlier reports (*2*, *20*). After some transformations Eq. [6] takes the form

$$-S(x_i, t_{k-1}) = \alpha D(x_i) S(x_{i+1}, t_k) - \left\{1 + \alpha(D(x_i) + D(x_{i-1})) - \left(\sqrt{-1}\gamma g(t_k) x_i - \frac{1}{T(x_i)}\right)\Delta t\right\} \times S(x_i, t_k) + \alpha D(x_{i-1}) S(x_{i-1}, t_k), \qquad [9]$$

where $\alpha = \Delta t/\Delta x^2$. The last expression is in fact a sequence of tridiagonal linear sets of equations which should be solved for each time step t_k, $k = 1, \ldots$, when the magnetization from the previous time step t_{k-1} is already known. Calculations start with the initial condition at time 0. The tridiagonal equation can be solved by the Gauss elimination method, adopted for tridiagonal sets (*23*), which provides high accuracy and speed of processing. Analogous sets of linear algebraic equations can be derived for the Crank–Nicholson scheme (Eq. [7]).

The Crank–Nicholson scheme is assumed to be second-order accurate in time, whereas the implicit scheme is only first-order (*24*). Our calculations, however, showed that in all cases, which will be introduced below, the results of these methods were hardly distinguishable, while the Crank–Nicholson algo-

rithm is approximately 30% slower than the implicit one. The developed computer program contains both opportunities as an option.

When the strength of the gradient pulse is high, the phase difference between adjacent positions can be very large, and in that case it is impossible to get sufficient accuracy with reasonable values for the time and space steps. If this is the case it is worthwhile to solve a linear set, assuming that there is no influence of the gradient pulse,

$$-S^*(x_i, t_{k-1}) = \alpha D(x_i) S^*(x_{i+1}, t_k) - \left\{1 + \alpha(D(x_i) + D(x_{i-1})) + \frac{1}{T(x_i)}\Delta t\right\} \times S^*(x_i, t_k) + \alpha D(x_{i-1}) S^*(x_{i-1}, t_k), \quad [10]$$

and then make the correction for the influence of the gradient pulse, multiplying the solution by the factor, characterizing the influence of the gradient pulse:

$$S(x_i, t_k) = S^*(x_i, t_k)\exp(\sqrt{-1}\gamma g(t_k) x_i). \quad [11]$$

However, even in this case, in order to get good accuracy, a sufficiently large number of time and space steps are required. This problem can be solved by modeling the gradient pulses with a time and space step much smaller than the time and space step in the time regions without gradient pulses, which results in higher accuracy without increasing the calculation time too much.

3. SOFTWARE IMPLEMENTATION

The numerical model was implemented using the programming language C++ as a DLL module, which can be used for a wide variety of different external software systems. On the input it requires a structure, containing parameters which determine the number of compartments, diffusion coefficient, decay time, length and membrane permeability for each compartment, characteristics of the gradient pulses, number of steps in the time and space domains, and method of modeling. On the output it yields the arrays of the magnetization amplitude and phase as it develops in time and space for a given value of the pulse field gradient amplitude. Input structure can be easily reprogrammed to encompass the different number of compartments, membrane permeabilities, characteristics of the gradient pulses, etc.

One of the advantages of the described model is its flexibility. It can be adopted for the modeling of other gradient pulse sequences, exploration of the influence of internal magnetic field gradients, and more complicated geometry of the compartments (nonplanar barriers). The problems of the extrapolation of this model into the second and third space dimensions are under consideration at the moment.

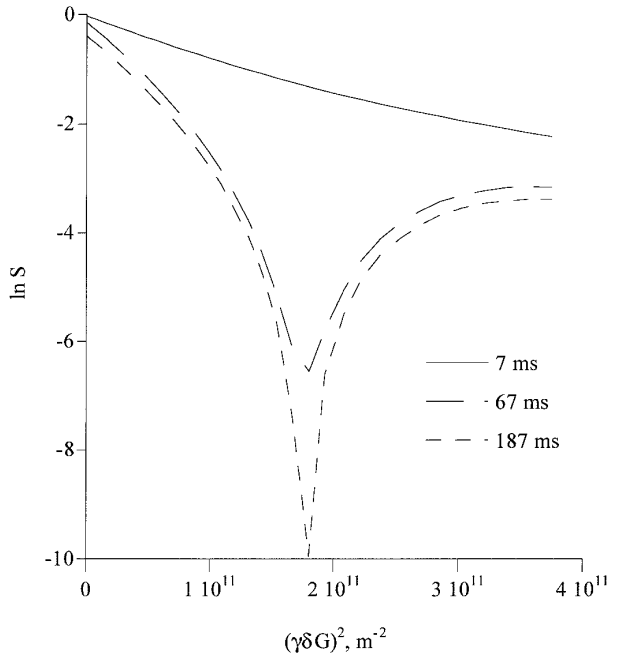

FIG. 3. Spin–echo attenuation plot for three values of Δ: 7, 67, and 187 ms. One compartment: length, 15 μm; diffusion coefficient, 2×10^{-9} m^2/s; the boundaries are fully reflective (total calculation time is about 18 s on an Indy Silicon Graphics WorkStation).

The implemented algorithm is fairly fast: for obtaining one value of the magnetization amplitude and phase (time region without gradient pulses), by the implicit method one needs only three complex operations of summation and multiplication and, of course, some preliminary actions, which, however, do not take much time. So calculation of the whole time–space surface (typically 256 time steps and 225 space steps) takes about 0.75 s on an Indy Silicon Graphics WorkStation. This fact gives us good hope to use this model for the development of a fitting routine for the estimation of the set of variables, describing compartments in terms of lengths and membrane permeabilities, and in addition diffusion coefficients and relaxation times from experimental pfg-CPMG systems.

4. RESULTS AND DISCUSSION

We performed many calculations with the numerical model in order to find a correspondence with results reported previously. We started with a one-compartment system with the geometry close to the geometry described in (*11*). The length of the compartment was set to 15 μm, the diffusion coefficient was equal to 2×10^{-9} m^2/s, and the boundaries were assumed to be fully reflective. The spin–echo attenuation plots for three values of Δ (7, 67, and 187 ms) are shown in Fig. 3. These plots were obtained

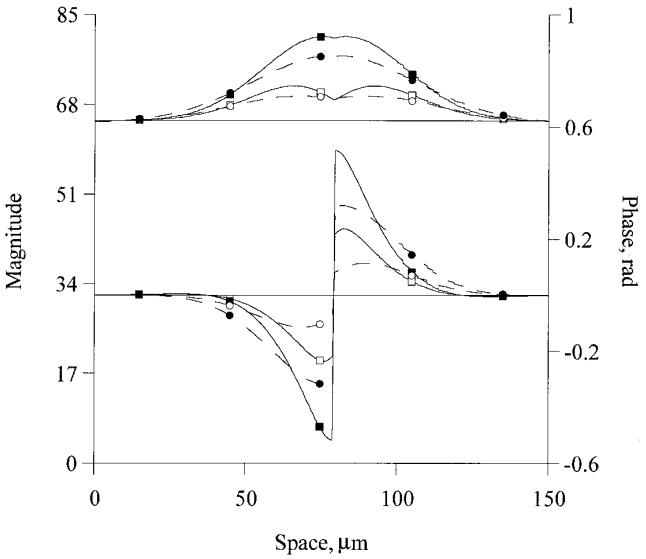

FIG. 4. Spatial distribution of magnetization magnitude and phase for two time instances, 120 ms (squares) and 160 ms (circles), and two values of membrane permeability, 1×10^{-4} m/s (empty points) and 1×10^{-5} m/s (filled points). Compartments have the same values for the diffusion coefficient, 2.5×10^{-9} m^2/s; time relaxation constant, 10 s; and length, 80 μm. Parameters of the magnetic field gradient pulses are $G = 14.1$ mT/m, $\delta = 10$ ms, $\Delta = 0.11$ s (total calculation time is about 1 s on an Indy Silicon Graphics WorkStation).

by integration over all space steps for different values of G and using an echo time directly after the gradient pulses ($\delta = 1$ ms). We obtained numerous dips, the abscissa of which corresponds to the width of the compartment. The first minimum, which is shown in the figure, is observed at $\gamma\delta G = 2\pi/L$. This result is in full accordance with results obtained in (*11*).

Several calculations were performed in order to find accordance with the numerical model reported in (*20*). A two-compartment system with a semi-permeable membrane and open output boundaries was modeled. Each compartment has the same value for the diffusion coefficient (2.5×10^{-9} m^2/s), relaxation time constant (10 s), and length (80 μm). The parameters of the magnetic field gradient pulses were $G = 14.1$ mT/m, $\delta = 10$ ms, $\Delta = 0.11$ s. In Fig. 4 the spatial distribution of the magnetization magnitude and phase immediately after the second gradient pulse (squares) and 40 ms later (rounds) for two values of permeability (1×10^{-4} m/s, empty points; 1×10^{-5} m/s, filled points) is presented. The observed result corresponds to the data, given in (*20*), for the same set of parameters. The important improvement of our model is presented in the same figure, where the time development of the magnitude and phase of the magnetization at each space position is shown. One can observe the further decrease of the amplitude and dispersion of the phase in time. A more complicated case is shown in the Fig. 5, where the time development of the magnetization magnitude and phase for a four-compartment system with open boundaries and semi-permeable membranes for four values of the gradient field strength is shown. One can clearly observe that the relative amplitude near the membranes builds up due to restricted diffusion and that the phase of the magnetization is affected by the permeability of the membranes. This change of the phase is caused by an imbalance of the spins moving to the right or left, which results in a flow-like phase buildup. Note that the net phase over the whole system is zero.

The next numerical experiment demonstrates the importance of the time domain in the NMR experiments. Two systems of the same length (3×10^{-5} m), consisting of two closed compartments (fully reflective walls), were modeled. Systems differ in the diffusion coefficients (for the first compartment, 2×10^{-9} and 4.5×10^{-10} m^2/s; for the second, 5×10^{-10} and 1.37×10^{-9} m^2/s) and lengths of compartments (for the first compartment, 2×10^{-5} and 5×10^{-6} m; for the second, 1×10^{-5} and 2.5×10^{-5} m). Relaxation times for each compartment were equal in both systems (for the first compartment, 1 s and for the second, 0.5 s). In Fig. 6 we present attenuation plots for these systems, and in Fig. 7 we present relaxation of the magnetization in time for three gradient pulse strength values $G = 0$, 0.658, and 1.41 T/m. In the system with the fully reflective walls, when the magnetic field gradient is absent ($G = 0$), one can observe only T_2 relaxation (Fig. 7 (1)). In this case magnetization from the second system (dashed line on the Fig. 7) is relaxing faster, because the contribution from the longest compartment (2.5×10^{-5} m) with the shortest relaxation time (0.5 s) in total relaxation is higher for this system. When increasing the gradient pulse strength, the diffusion process becomes more pronounced, and for $G = 1.41$ T/m (Fig. 7 (3)) the total relaxation of the second system becomes slower than that of the first one, since in the first system the longest compartment has the greatest diffusion coefficient. Such different behavior is noticeable only at longer echo times, and it is practically impossible to discriminate between the two systems, judging only by the spin–echo attenuation plot (Fig. 6), measured with a signal-to-noise ratio of 1000 immediately after the second gradient pulse (random noise added to spin–echo attenuation plot was generated by a special software generator in order to simulate the influence of experimentally detected statistical distortions). This problem may be relevant for fitting procedures, where the time domain becomes an extremely important source of information for diffusion and structural properties of the explored substance.

5. CONCLUSION

Further development of the numerical model of restricted diffusion and magnetization relaxation behavior in pulsed field gradient pfg-CPMG NMR experiments was presented. The model allows for easy changes in the number of compartments, compartment size, diffusion and intrinsic relaxation times in the compartments, membrane permeabilities, etc. A number of

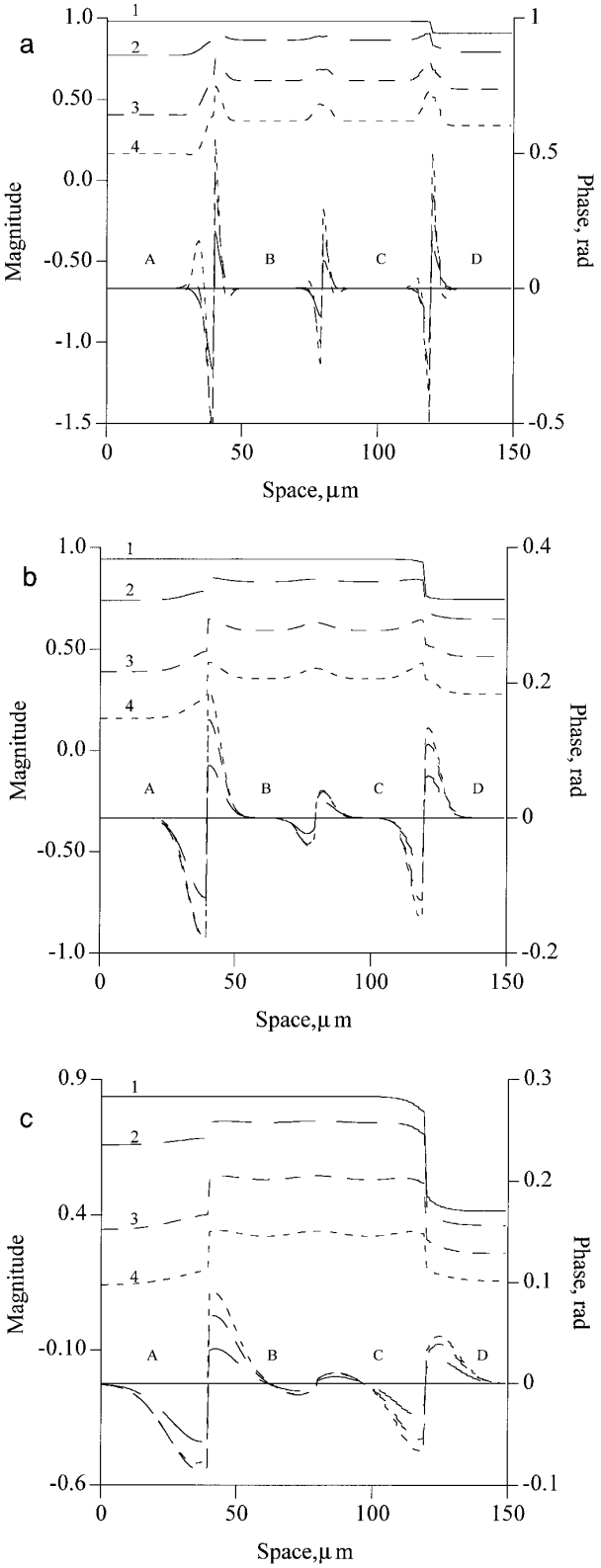

FIG. 5. Time development of magnetization magnitude and phase for a four-compartment system with open boundaries and semi-permeable membranes for four values of gradient field strength: $G = 0$ T/m (1); 0.705 T/m (2); 1.41 T/m (3); 1.845 T/m (4); $\delta = 1$ ms, $\Delta = 7$ ms. Echo time: 8 ms (a); 40 ms (b); 80 ms (c) (total calculation time is about 3 s on an Indy Silicon Graphics WorkStation). Compartment parameters: A, $D = 1 \times 10^{-9}$ m^2/s; $T = 0.5$ s. B, $D = 0.5 \times 10^{-9}$ m^2/s; $T = 0.5$ s C: $D = 0.5 \times 10^{-9}$ m^2/s; $T = 0.5$ s. D, $D = 0.5 \times 10^{-9}$ m^2/s; $T = 0.1$ s. Permeabilities: between A and B, 1×10^{-5} m/s; between B and C, 1×10^{-4} m/s; between C and D, 2×10^{-5} m/s.

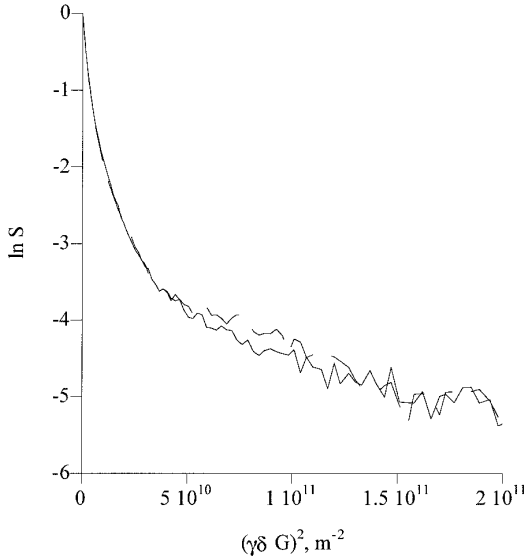

FIG. 6. Spin–echo attenuation plot for two systems (signal-to-noise ratio 1000). (a) One-compartment: $D = 2 \times 10^{-9}$ m^2/s, $T = 1$ s, $L = 2 \times 10^{-5}$ m; two-compartment: $D = 5 \times 10^{-10}$ m^2/s, $T = 0.5$ s, $L = 1 \times 10^{-5}$ m (solid line). (b) One-compartment: $D = 4.5 \times 10^{-10}$ m^2/s, $T = 1$ s; $L = 5 \times 10^{-6}$ m; two-compartment: $D = 1.37 \times 10^{-9}$ m^2/s; $T = 0.5$ s; $L = 2.5 \times 10^{-5}$ m (dashed line). (Total calculation time is about 14 s on an Indy Silicon Graphics WorkStation.)

numerical experiments were performed, which prove the correctness of the implemented model and correspondence to the previously obtained results. At the same time the presented model significantly expands the range of explored configurations, allowing us to forecast the behavior of a system using different spin–echo sequences, study the influence of instrumental distortions, and look into the development of the magnetization in the time.

The latter is very important from an experimental point of view. As we have shown, the time domain contains valuable information which is now accessible by experiment (*21*). Two domain data sets (echo time and gradient strength) obtained in the experiment have to be fitted then in terms of membrane permeabilities, length of compartments, diffusion coefficients, and relaxation times. This model is a good starting point for the development of such fitting procedures based on a global approach. This possibility is supported by the very good speed properties of the implemented software. The information about the membrane permeabilities and length of compartments, as

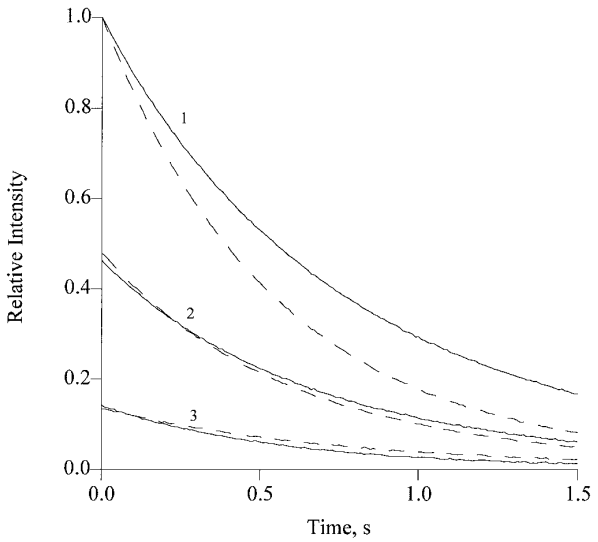

FIG. 7. Time development of magnetization for two systems (see caption for Fig. 6) for three values of gradient field strength: $G = 0$ T/m (1); 0.658 T/m (2); 1.41 T/m (3) (total calculation time is about 2 s on an Indy Silicon Graphics WorkStation).

well as diffusion coefficients, and relaxation times which can be extracted by a fitting procedure, could be very important for further development of the pfg NMR technique.

The presented numerical model can be further extended to simulate two-dimensional diffusion (manuscript in preparation). Preliminary work has been done in this way, indicating that it did not introduce any principal obstacles. First test calculations with a model consisting of concentric cylinders resulted in an increase in calculation time of a factor of about five. These results indicate the feasibility to build more adequate models describing a variety of biological objects and porous networks.

REFERENCES

1. P. T. Callaghan, *J. Magn. Reson. A* **113,** 53 (1995).
2. B. P. Hills and J. E. M. Snaar, *Mol. Phys.* **76,** 979 (1992).
3. P. P. Mitra and N. Sen, *Phys. Rev. B* **45,** 143 (1992).
4. J. Kärger and W. Heink, *J. Magn. Reson.* **51,** 1 (1983).
5. D. G. Cory and A. N. Garroway, *Magn. Reson. Med.* **14,** 435 (1990).
6. P. T. Callaghan, D. MacGowan, K. J. Packer, and F. O. Zelaya, *J. Magn. Reson.* **90,** 177 (1990).
7. B. Balinov, B. Jönsson, P. Linse, and O. Söderman, *J. Magn. Reson. A* **104,** 17 (1993).
8. P. Linse and O. Söderman, *J. Magn. Reson. A* **116,** 77 (1995).
9. H. Gudbjartsson and S. Patz, *IEEE Trans. Med. Imag.* **14,** 636 (1995).
10. E. O. Stejskal and J. E. Tanner, *J. Chem. Phys.* **42,** 288 (1965).
11. J. E. M. Snaar and H. Van As, *J. Magn. Reson. A* **102,** 318 (1993).
12. A. V. Barzykin, K. Hayamizu, W. S. Price, and M. Tachiya, *J. Magn. Reson. A* **114,** 39 (1995).
13. A. Caprihan, L. Z. Wang, and E. Fukushima, *J. Magn. Reson. A* **118,** 94 (1996).
14. P. P. Mitra and B. I. Halperin, *J. Magn. Reson. A* **113,** 94 (1995).
15. P. W. Kuchel, A. J. Lennon, and C. Durrant, *J. Magn. Reson. B* **112,** 1 (1996).
16. A. Caprihan, L. Z. Wang, and E. Fukushima, *J. Magn. Reson. A* **118,** 94 (1996).
17. J. Crank, "The Mathematics of Diffusion," Oxford Univ. Press, London (1975).
18. K. R. Brownstein and C. E. Tarr, *Phys. Rev. A* **19,** 2446 (1979).
19. V. M. Kenkre, E. Fukushima, and D. Sheltraw, *J. Magn. Reson. A* **128,** 62 (1997).
20. T. A. Zawodzinski, T. E. Springer, M. Neeman, and L. O. Sillerud, *Israel J. Chem.* **32,** 281 (1992).
21. D. van Dusschoten, C. T. W. Moonen, P. A. de Jager, and H. Van As, *Magn. Reson. Med.* **36,** 907 (1996).
22. T. Meis and U. Marcowitz, "Numerical Solution of Partial Differential Equations," Springer-Verlag, New York/Heidelberg/Berlin (1981).
23. G. E. Forsythe and W. R. Wasow, "Finite-Difference Methods for Partial Differential Equations," Wiley, New York (1965).
24. W. H. Press, B. P. Flannery, S. A. Teukolsky, and W. T. Vetterling, "Numerical Recipes in C. The Art of Scientific Computing," Cambridge Univ. Press, Cambridge, UK (1988).